



ELSEVIER

Contents lists available at ScienceDirect

# Engineering Failure Analysis

journal homepage: [www.elsevier.com/locate/engfailanal](http://www.elsevier.com/locate/engfailanal)

## Numerical analysis and discussion on the hot-spot stress concept applied to welded tubular KT joints

Bianca Vieira Ávila<sup>a,\*</sup>, José Correia<sup>b,c</sup>, Hermes Carvalho<sup>d</sup>, Nicholas Fantuzzi<sup>e</sup>,  
Abílio De Jesus<sup>f</sup>, Filippo Berto<sup>g</sup>

<sup>a</sup> Federal University of Minas Gerais, Belo Horizonte, Brazil

<sup>b</sup> INEGI & CONSTRUCT, Faculty of Engineering, University of Porto, 4200-465 Porto, Portugal

<sup>c</sup> Faculty of Civil Engineering and Geosciences, Delft University of Technology, 2600 GA Delft, the Netherlands

<sup>d</sup> Federal University of Minas Gerais, Belo Horizonte, Brazil

<sup>e</sup> DICAM Department, University of Bologna, Viale del Risorgimento 2, 40136 Bologna, Italy

<sup>f</sup> INEGI, Faculty of Engineering, University of Porto, 4200-465 Porto, Portugal

<sup>g</sup> Department of Mechanical and Industrial Engineering, Norwegian University of Science and Technology, Richard Birkelands vei 2b, 7491 Trondheim, Norway

### ARTICLE INFO

#### Keywords:

Tubular joints  
Hot-spot stress  
Analytical solutions  
Finite element analysis  
Extrapolation method

### ABSTRACT

Nominal stresses have been used for a long time for the assessment of fatigue resistance of welded joints, however, this approach has strong limitations since the definition of the nominal stress may be subjective for complex welded details and/or complex loading. On the other hand, the hot-spot stress approach has been proposed to overcome these limitations considering the structural geometrical discontinuities.

However, the hot-spot stress methods also present certain limitations, and the present study aims at evaluating the available numerical and analytical hot-spot stress methods proposed by DNVGL (2016) and IIW (2014). The particular case of an offshore tubular KT joint has been considered herein and discretized in two planes. It has been studied numerically using the ABAQUS software coupled with the hot-spot stress extrapolation methods described in IIW (2014) and DNVGL (2016). The influence of the weld geometry has been considered and evaluated. In addition to the numerical method, the present study has also considered the analytical approach proposed in DNVGL (2016) derived from the combination of Efthymiou solutions for the stress concentration factor with the method of superposition of stresses. The numerical models according to IIW (2014) have been found to be more conservative when compared with the mesh-size methods proposed by DNVGL (2016), both in numerical modelling without the weld or with weld. For the numerical models with weld cord, the mean values of normalized difference index obtained for all braces together, as a result of comparing numerical results with analytical solutions, are lower, when compared with results obtained from the numerical models without weld cord.

\* Corresponding author.

E-mail addresses: [bianca.avila@ufmg.br](mailto:bianca.avila@ufmg.br) (B. Vieira Ávila), [jacorreia@inegi.up.pt](mailto:jacorreia@inegi.up.pt), [J.A.FonsecadeOliveiraCorreia@tudelft.nl](mailto:J.A.FonsecadeOliveiraCorreia@tudelft.nl) (J. Correia), [hermes@dees.ufmg.br](mailto:hermes@dees.ufmg.br) (H. Carvalho), [nicholas.fantuzzi@unibo.it](mailto:nicholas.fantuzzi@unibo.it) (N. Fantuzzi), [ajesus@fe.up.pt](mailto:ajesus@fe.up.pt) (A. De Jesus), [filippo.berto@ntnu.no](mailto:filippo.berto@ntnu.no) (F. Berto).

<https://doi.org/10.1016/j.engfailanal.2022.106092>

Received 31 October 2021; Received in revised form 13 January 2022; Accepted 19 January 2022

Available online 4 February 2022

1350-6307/© 2022 Elsevier Ltd. All rights reserved.

**List of Notation**

$d$	member diameter
$g_{AB}$	gap between brace A and brace B
$g_{BC}$	gap between brace B and brace C
$R$	external radius of the chord
$r$	external radius of the brace
$T$	chord thickness
$t$	brace thickness
IIW	International Institute of Welding
DNVGL	Det Norske Veritas and Germanischer Lloyd
$SCF$	stress concentration factor
$SCF_{AC}$	stress concentration factor at the crown for axial load
$SCF_{AS}$	stress concentration factor at the saddle for axial load
$SCF_{MIP}$	stress concentration factor for in plane moment
$SCF_{MOP}$	stress concentration factor for out of plane bending
$\theta_A$	angle between brace A and chord
$\theta_B$	angle between brace B and chord
$\theta_C$	angle between brace C and chord
$\sigma_{hs}$	hot-spot stress
$\sigma_{loc}$	notch stress
$\sigma_{nom}$	nominal stress
$\sigma_x$	maximum nominal stresses due to axial load
$\sigma_{my}$	maximum nominal stresses due to in-plane bending
$\sigma_{mz}$	maximum nominal stresses due to out-plane bending

**1. Introduction**

Jacket-type support structures are one of the most common types of offshore support structures representing 95% of fixed offshore structures [1]. These structures are preferred when the sea depth becomes moderate to deep, when compared to other fixed support structures such as monopile foundations [2]. The main type of loading which these structures are submitted to is due to the sea waves that have characteristics of stochastic events [3,4].

The most common failure mode in jacket support structures is due to fatigue damage, which occurs as a result of accumulated damage [5,6]. Generally, fatigue failure occurs in welded members due to the stress concentrations resulting from local changes in geometry and the presence of welding; failures in these regions could occur even if the stresses in the critical regions are lower than the elastic limit [7,8]. The calculation of the fatigue life in welded tubular joints is often based on the S-N curves based-approaches [9]. Codes and recommendations such as those from the International Institute of Welding - IIW [10] and DNVGL [11] provide global fatigue damage approaches, based on S-N curves, to be applied to welded joints, the latter being specific for offshore structures. Shabakhty et al. [12] presented a discussion on the fatigue resistance modelling based on the fracture mechanics (FM) based-approach, where a comparison between the obtained S-N curves following two standards, DNVGL-RP-C203 [11] and API-RP2A-WSD [13], was done. These authors concluded that to obtain better fitting with the S-N curves, calibration factors are needed, and, therefore, these factors have been proposed. Currently, several approaches are present in the literature to estimate the fatigue life, such as the local approach proposed by Mourão et al. [14] based on Neuber's rule [15] combined with the Ramberg–Osgood description [16] and Coffin-Manson [17,18,19] damage model. Nubuco et al. [20] performed fatigue loading (actions) estimations on an offshore jacket structure based on operational modal expansion analysis.

When performing finite element (FE) simulations, depending on the loads and geometries, it may be difficult to define the nominal stress to be used together with the S-N curve. In this case, it is more convenient to extract hot-spot stress (HSS) from the analysis than that of nominal stress [11]. In jacket-type offshore structures, the HSS occurs in the joint's regions around the circumference of the weld, where there are geometric discontinuities and consequently stress concentrations.

In several studies, the hot-spot stress method has been used to verify fatigue life prediction of different types of steel tubular joints. In 1970, studies on new fatigue approaches based on S-N curves and hot-spot stresses have intensified. As these studies expanded, it was clear that the analysis of stress concentration factors (SCFs) was essential for the fatigue life estimation of nodal joints. The first studies about these factors applied to offshore tubular joints were developed by Toprac and Beale [21] who founded a limited database of experimental steel joints. The high costs demanded by the experimental tests led Reber [22], Visser [23], and Kuang et al. [24] to use finite element analyses based on shell models to study stress concentrations in welded cylindrical joints [25]. Potvin et al. [26] numerically evaluated the stress concentration factor in K, T, and KT tubular joints. In this study, hot-spot stresses were admitted as the stress immediately at the weld toe without consideration of the extrapolation method. Efthymiou [27] developed a set of parametric equations to obtain the SCF applied to simple tubular joints of type T, Y, X, K, and KT, subjected to axial loads, in-plane and out-of-plane bending loads. These equations are applied and recommended by the DNVGL-RP-C203 code [11].

The models of tubular joints with weld representation have been studied since Efthymiou [27], but unfortunately few comparative studies demonstrating the influence of welds on fatigue stresses are available. Recently, Hectors and De Weale [28] assessed the influence of weld penetration according to AWS D1.1 guidelines [29]. The models included a shell model, a solid model without weld geometry, a solid model with a minimized weld geometry, and a solid model with maximized weld geometry. The results show that the geometry of the weld has a strong influence in the magnitude of the critical stress concentration factor.

The hot-spot stress method for a weld can be determined by either linear or quadratic extrapolations from surface stresses nearby the weld region. These extrapolation procedures are defined in design guidelines such as CIDETC Design Guide No. 8 [30], IIW [10], and DNVGL-RP-C203 [11]. IIW [10] establishes extrapolation methods in detail for weld members in general, while the DNVGL-RP-C203 [11] has specific guidelines for obtaining hot-spot stresses through the extrapolation method in offshore tubular joints.

Haghpanahiand and Pirali [31] estimated the HSS for a Tubular T-Joint under combined axial and bending loading. Therefore, the stress concentration factors for axial loading and in-plane bending loading were calculated using different parametric equations and finite element methods through an extrapolation method. The HSS distributions around the intersection were verified by the results obtained from the API RP2A Code procedure [13]. Yin et al. [32], Bao et al. [33,34,35] also determined the HSS based on the results of finite element analysis by extrapolation method in tubular offshore joints. Recently, new methods have been proposed to evaluate hot-spot stresses in offshore welded joints such as the analytical methods proposed by Oshogbunu et al. [36,37] whose equations were developed from regression of the results of an extensive parametric study of DKK joints.

Larsen et al. [2] estimated the fatigue life of the K-type joint of an offshore jacket; in this study three finite element models of different weld geometries were calibrated from an experimental model. One of the numerical models was built using the real 3D digitized weld geometry, another with the weld geometry proposed by offshore design codes, and the third model without any weld geometry representation. The results showed that the models with the 3D digitized welds provided the deformation ranges with more accuracy, while the FE models with the recommended weld geometry from the design codes were less accurate. The authors concluded that the 3D digitized weld geometry or the DNVGL recommendation for modelling the weld should be included in the FE models for tubular joints.

Aidibi et al. [38] presented a comparative study between Efthymiou's analytical formulations and numerical solutions by finite element analysis (FEA), considering the hot-spot stress approach recommended by IIW, to evaluate the stress concentration factor (SCF) of offshore tubular KT joints. In this research work, the authors concluded that the SCFs estimated by FEA at the crown points of the main chord have shown very high values when compared with DNVGL (Efthymiou's relations). These authors also suggested that a study including welds needs to be done to understand the behaviour of welds in KT tubular joints.

The present study intends to evaluate the hot-spot stresses in a critical tubular KT joint of an offshore structure. The critical tubular KT joint was identified from dynamic analyzes and fatigue assessment carried out by Mourão [39]. The mesh-size and extrapolation methods proposed by IIW [10] and DNVGL-RP-C203 [11] are applied in the numerical models and evaluated in comparison to the Efthymiou solutions aiming at obtaining the hot-spot stresses (HSS) also described in DNVGL-RP-C203 [11]. In both numerical models, the influence of the weld geometry is considered and evaluated. These methodologies are applied for KT joints which are part of an offshore jacket-type platform. Real wave loads were studied into 24 steps over time using static analysis. Axial loads, in-plane and out-of-plane bending were applied simultaneously to the joint braces.

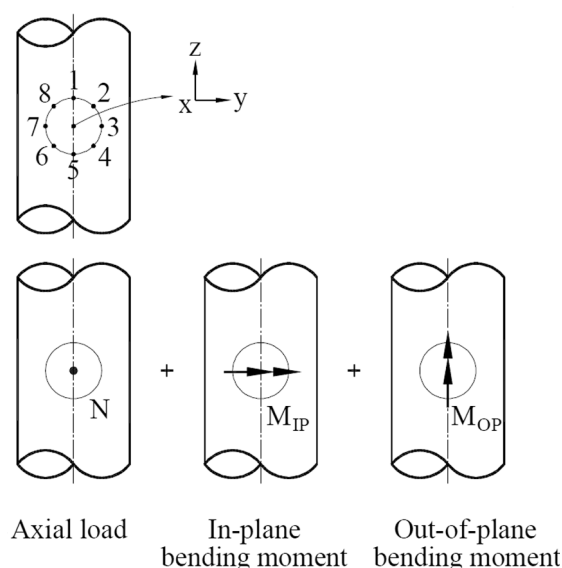


Fig. 1. Superposition of stresses from different load components (DNVGL-RP-C203 recommended practice [11]).

## 2. Stress concentration factor and hot-spot stress for tubular joints

The effect of geometric discontinuities in welded tubular joints induces changes in the stresses field. For this reason, stress concentrations near the weld regions are generated. In these stress concentration regions, the structure is more susceptible to fatigue damage. The concept of the stress concentration factor,  $SCF$ , is introduced as a ratio between the notch stress ( $\sigma_{loc}$ ) or hot-spot stress ( $\sigma_{hs}$ ) and nominal stress ( $\sigma_{nom}$ ), is given by Equation (1):

$$SCF = \frac{\sigma_{loc}}{\sigma_{nom}} \text{ OR } \frac{\sigma_{hs}}{\sigma_{nom}} \tag{1}$$

The DNV-RP-C203 [11] establishes recommendations for the fatigue design of offshore steel structures. The code provides the equations developed by Efthymiou for calculating the SCFs. The Efthymiou solutions [11,27] were obtained by finite element modelling using 3-dimensional shell elements. The SCFs were obtained using the hot-spot stress approach from the maximum principal stresses linearly extrapolated to the modelled weld toe through diagonal elements. Efthymiou’s formulations based on finite element analysis (FEA) lead, in most cases, to results that are underpredicted to those frequently observed, since they have a smaller number of conservative assumptions [27]. The stress concentration factors are calculated at 8 different points around the intersection circumference between the braces and chord (see Fig. 1), in order to identify the location where the stress concentration is the highest.

### 2.1. Superposition of stresses in tubular joints – analytical method

According to DNV-RP-C203 [11], the stresses in tubular joints due to brace loads are calculated at the crown and the saddle points. Then, the hot spot stresses at these points are derived by summation of the single stress components from axial, in-plane, and out-of-plane loadings. The resulting hot-spot stresses at eight positions can be derived by the superposition of stresses due to axial force, in-plane loading, and out-of-plane loading. The structural stresses around the weld are given by Equations (2) to (9):

$$\sigma_1 = SCF_{AC}\sigma_x + SCF_{MIP}\sigma_{my} \tag{2}$$

$$\sigma_2 = \frac{1}{2}(SCF_{AC} + SCF_{AS})\sigma_x + \frac{1}{2}\sqrt{2}SCF_{MIP}\sigma_{my} - \frac{1}{2}\sqrt{2}SCF_{MOP}\sigma_{mz} \tag{3}$$

$$\sigma_3 = SCF_{AS}\sigma_x + SCF_{MOP}\sigma_{mz} \tag{4}$$

$$\sigma_4 = \frac{1}{2}(SCF_{AC} + SCF_{AS})\sigma_x - \frac{1}{2}\sqrt{2}SCF_{MIP}\sigma_{my} - \frac{1}{2}\sqrt{2}SCF_{MOP}\sigma_{mz} \tag{5}$$

$$\sigma_5 = SCF_{AC}\sigma_x - SCF_{MIP}\sigma_{my} \tag{6}$$

$$\sigma_6 = \frac{1}{2}(SCF_{AC} + SCF_{AS})\sigma_x - \frac{1}{2}\sqrt{2}SCF_{MIP}\sigma_{my} + \frac{1}{2}\sqrt{2}SCF_{MOP}\sigma_{mz} \tag{7}$$

$$\sigma_7 = SCF_{AS}\sigma_x + SCF_{MOP}\sigma_{mz} \tag{8}$$

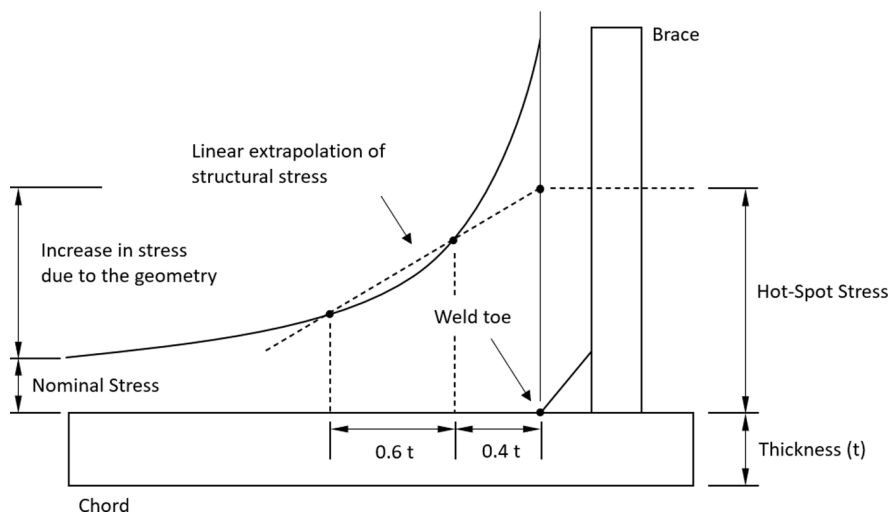


Fig. 2. Extrapolation of hot spot stress according to IIW (Adapted from Lee [40]).

$$\sigma_8 = \frac{1}{2}(SCF_{AC} + SCF_{AS})\sigma_x + \frac{1}{2}\sqrt{2}SCF_{MP}\sigma_{my} + \frac{1}{2}\sqrt{2}SCF_{MOP}\sigma_{mz} \quad (9)$$

where

- $\sigma_x, \sigma_{my}$  and  $\sigma_{mz}$  are the maximum nominal stresses due to axial load and in-plane and out-plane moments, respectively;
- $SCF_{AS}$  and  $SCF_{AC}$  are the stress concentration factors at the saddle and crown for axial load and;
- $SCF_{MP}$  and  $SCF_{MOP}$  are the stress concentration factors for in-plane and out-of-plane bending moments, respectively.

### 3. Mesh-size and extrapolation methods for hot-spot stress analysis

#### 3.1. IIW guidelines

In numerical models, the hot-spot stress can be determined using reference points by extrapolation to the weld toe under consideration from stresses at reference points. If the weld is not modelled, the IIW [10] recommends that extrapolation to the structural intersection point is necessary to avoid stress underestimation due to the missing stiffness of the weld. In this method, the finite element lengths are determined by the reference points selected for stress evaluation, i.e. the element size at the hot spot corresponds to its distance from the first reference point. IIW [10] allows determining the structural hot spot stress using the reference points and extrapolation equations for different mesh sizes and extrapolation orders. In this study, it was considered a fine mesh with an element size not more than  $0.4t$  and linear extrapolation. Thus, the obtained nodal principal stresses must be at two reference points located at a distance of  $0.4t$  and  $1.0t$  from the weld toe or intersections (see Fig. 2), where  $t$  is the thickness of the tube. For this condition, the hot-spot stresses can be evaluated by Equation (10):

$$\sigma_{hs} = 1.67\sigma_{0.4t} - 0.67\sigma_{1.0t} \quad (10)$$

#### 3.2. DNVGL guidelines

DNVGL-RP-C203 [11] as well as IIW [10] provide guidelines for obtaining the numerical hot-spot stress. However, DNVGL has specific conditions for tubular joints for offshore structures. The structural stress can be obtained by linear extrapolation of the stresses obtained from nodal points at a certain distance from the weld toe as shown in Fig. 3 and Table 1.

### 4. Numerical study of a tubular KT-joint

A tubular KT-joint will be modelled based on FE solid modelling. Solid models, with and without welds representation, were evaluated thru a linear finite element analysis using the ABAQUS 6.14 software [41]. Previous analyses carried out on the initial models in the research by Mourão et al. [14,39] showed that the maximum stresses obtained from dynamic analyses were considerably lower than the yield stresses (420 MPa) of the S420 steel taken as the base analysis according to the DNVGL-RP-C208 standard [11]. In this research, this result was also observed since the maximum hot-spot stress amplitudes presented in Section 5 (Fig. 13) were smaller

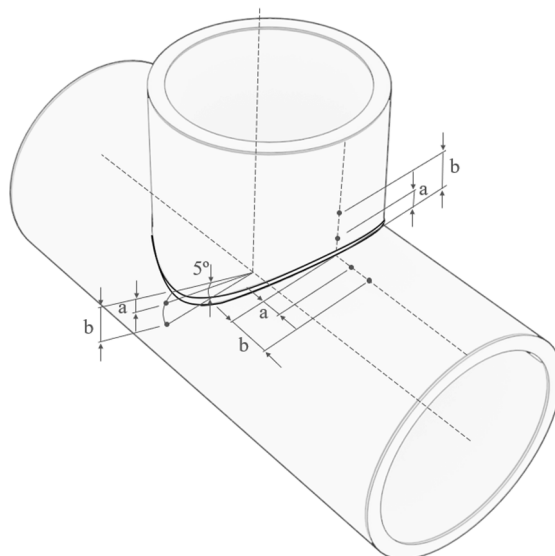


Fig. 3. Extrapolation of hot spot stress according to DNVGL-RP-C203 [11].

**Table 1**  
References Points.

Points	Brace Surface	Chord Surface - Crown	Chord Surface - Saddle
a	$0.2\sqrt{rt}$	$0.2\sqrt{rt}$	$0.2\sqrt{rt}$
b	$0.65\sqrt{rt}$	$0.4\sqrt{rtRT}$	$\pi R/36$

R: is the chord inner radius; r: is the bracing inner radius; T: is the chord wall thickness; t: it the bracing wall thickness.

than the yield stress by a factor of 3 times. Thus, considering a non-linear elastoplastic model would imply computationally heavier analyses, and, therefore a linear analysis was adopted. Also, code based S-N approaches for welded joints are usually based on elastic stress analysis, even in the case the stresses could increase beyond the yield stress. Furthermore, Young’s modulus and Poisson’s ratio were considered to be 210 GPa and 0.3, respectively. The finite elements adopted for analysis consisted of a 8-noded three-dimensional solid element with reduced integration (C3D8R).

4.1. Geometrical parameters

Two KT joints making part of a jacket-type structure located in the North Sea are evaluated. The joints are in different planes denominated as XZ and YZ planes. The YZ plane includes the main chord and braces 4938, 4940, and 4939; the XZ plane includes of the main chord and braces 5112, 5116, and 5110, as defined in Fig. 4 and Table 2.

Some simplifications in the weld geometry were adopted to make it possible to create a weld profile. The methodologies utilized by Yaghin and Ahmadi [42], Lee [40], and Chiew et al. [43] are used in the present research. The weld profile was modelled as a triangular fillet around the braces with a base and height equal to the thickness of the respective brace, as shown in Fig. 5.

4.2. Load analysis and boundary conditions

In the studies carried out by Mourão et al. [14,39], a global structural analysis of the jacket-type offshore platform using wave loading was performed. The global structure consists of a 140.3 m high offshore jacket (an elevation of 27 m above sea level and a water depth of 113.3 m). The global dynamic analysis of the structure under wave loading took into account wave measurements in the North Sea - wave scatter diagram that correlates wave periods, wave height, and the number of occurrences. The wave loads applied to tubular members of the structural model were calculated using fifth-order Stokes wave theory and Morrison’s formula [44]. From the study of a wave dispersion diagram, 8 waves with a probability of occurrence greater than 0.01% were analyzed. The 8 waves were evaluated in 12 different directions. In total 96 waves were studied in 24 steps overtime each wave. Of these 96 waves, the loading of a wave was identified that resulted in higher nominal stress in the critical joint under analysis. For this reason, this study will perform a static analysis of the 24 steps referring to wave 80. The loads used in this research are presented in Tables 3 and 4, for the YZ and XZ planes, respectively.

As for the boundary conditions, restrictions on displacements and rotations on the x, y, and z axes were applied to the ends of the main chord. Since Efthymiou’s formulations are independent of the boundary conditions of the end of the chord as mentioned by Saini et al. [45], it is possible to state that the conditions adopted do not interfere with the analytical–numerical comparative results.

4.3. Mesh and extrapolation method

To evaluate the extrapolation methods of the DNVGL-RP-C203 [11] and IIW recommendations [10], two different mesh compositions were built. The finite elements in each brace had a size indicated by ‘a’ for the mesh of DNVGL and by ‘0.4 t’ for the mesh of IIW. Thus, the extrapolation points and finite element size for the meshes under study are shown in Table 5. It should be noted that the mesh

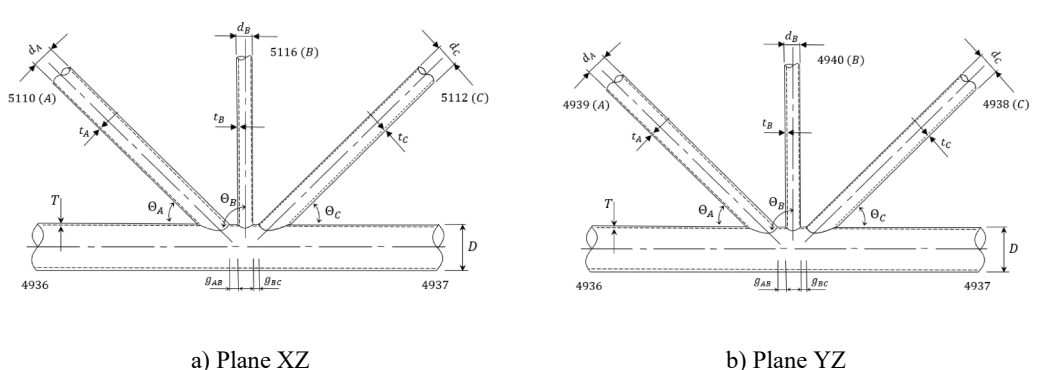


Fig. 4. XZ and YZ planes of the KT joint (DNVGL-RP-C203 [11]).

**Table 2**  
Dimensions of the KT joint for both planes.

	Member	$\theta$	$d$ (m)	$t$ (m)	$g_{AB}$ (m)	$g_{BC}$ (m)
Plane XZ	5110 (A)	38.418°	1.200	0.040	0.352	0.0726
	5116 (B)	90°	1.000	0.030		
	5112 (C)	38.416°	1.100	0.025		
Plane YZ	4939 (A)	30.119°	1.200	0.035	0.379	0.0747
	4940 (B)	83.231°	1.320	0.055		
	4938 (C)	43.665°	1.100	0.025		
Chord	4936	0°	2.300	0.095	-	-
	4937	0°	2.300	0.095	-	-

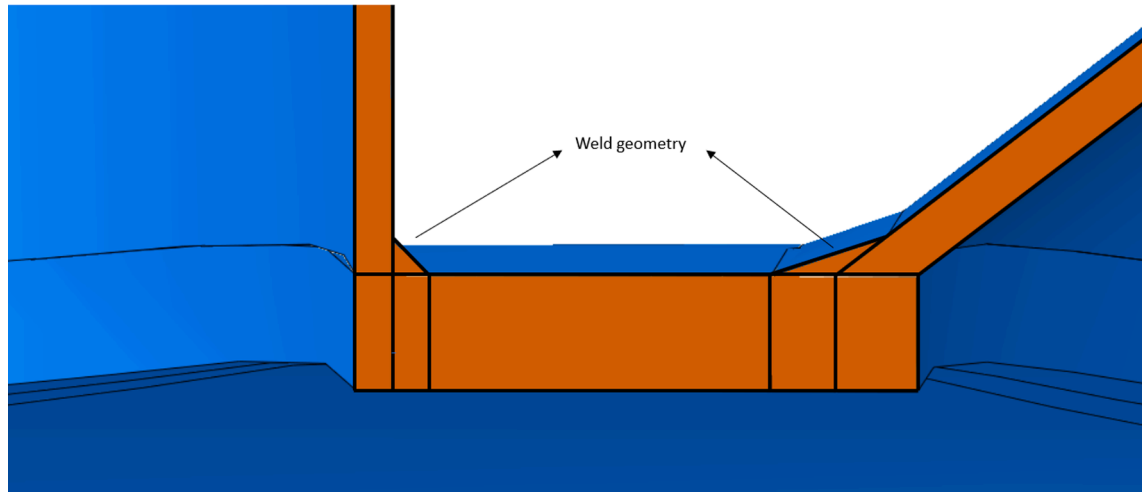


Fig. 5. Weld geometry.

**Table 3**  
Load cases in the braces of the YZ plane (Units:  $P_x$  in N,  $M_y$  and  $M_z$  in N.mm).

Step	Brace 4938			Brace 4939			Brace 4940		
	$P_x$	$M_y$	$M_z$	$P_x$	$M_y$	$M_z$	$P_x$	$M_y$	$M_z$
1	1,641,000	-126600000	-293000	-2040000	13,670,000	57,570,000	62,790	-827500000	93,620,000
2	1,063,000	-127700000	9,444,000	-1495000	-92830000	53,330,000	96,010	-777500000	44,180,000
3	327,000	-123700000	20,300,000	-743800	-198500000	44,960,000	125,800	-682000000	-14940000
4	-400200	-110200000	30,590,000	5930	-284700000	33,630,000	144,800	-570000000	-76790000
5	-956900	-85030000	39,440,000	547,600	-335400000	21,250,000	153,700	-461100000	-136800000
6	-1337000	-50880000	45,720,000	909,900	-348700000	7,921,000	147,200	-349400000	-187800000
7	-1576000	-12980000	49,090,000	1,139,000	-353400000	-5593000	134,500	-226400000	-225400000
8	-1700000	22,520,000	49,490,000	1,269,000	-359200000	-18260000	121,600	-91050000	-246700000
9	-1720000	49,770,000	47,310,000	1,313,000	-358400000	-28970000	110,600	49,670,000	-252000000
10	-1656000	64,590,000	43,230,000	1,287,000	-341500000	-37150000	93,480	184,600,000	-243500000
11	-1504000	69,570,000	37,630,000	1,191,000	-300100000	-42560000	68,630	295,300,000	-223600000
12	-1252000	73,750,000	30,650,000	1,006,000	-232200000	-44860000	37,130	363,200,000	-193200000
13	-896300	77,200,000	22,410,000	726,800	-142500000	-43770000	2042	378,100,000	-152900000
14	-449200	76,880,000	13,180,000	361,400	-41750000	-39310000	32,840	345,700,000	-103900000
15	62,860	69,690,000	3,481,000	-71850	56,480,000	-31750000	62,910	283,100,000	-48340000
16	596,800	53,510,000	-5890000	-541600	137,300,000	-21580000	82,820	201,500,000	9,875,000
17	1,098,000	27,840,000	-14010000	-1004000	187,100,000	-9501000	89,410	103,500,000	65,850,000
18	1,514,000	-5530000	-20090000	-1411000	202,800,000	3,726,000	81,990	-9727000	114,500,000
19	1,852,000	-41950000	-23790000	-1772000	210,500,000	17,330,000	70,310	-143400000	152,000,000
20	2,123,000	-75560000	-25040000	-2100000	220,100,000	30,500,000	60,760	-297700000	176,200,000
21	2,309,000	-101000000	-23970000	-2373000	223,600,000	42,020,000	52,500	-462200000	185,700,000
22	2,395,000	-114300000	-20940000	-2555000	211,000,000	50,970,000	37,960	-621100000	181,400,000
23	2,410,000	-117100000	-16200000	-2703000	174,500,000	55,760,000	9880	-760400000	163,800,000
24	2,167,000	-120900000	-9090000	-2555000	107,700,000	57,840,000	29,590	-834700000	133,700,000

**Table 4**  
Load cases in the braces of the XZ plane (Units: P<sub>x</sub> in N, M<sub>y</sub> and M<sub>z</sub> in N.mm).

Step	Brace 5110			Brace 5112			Brace 5116		
	Px	My	Mz	Px	My	Mz	Px	My	Mz
1	-874200	-167700000	-321200000	509,800	14,810,000	76,850,000	261,900	-94510000	-41630000
2	-801300	-219700000	-270600000	437,500	5,609,000	57,200,000	254,100	-99790000	-35010000
3	-614600	-263500000	-197300000	316,100	-6720000	32,600,000	201,700	-97840000	-27910000
4	-390100	-290000000	-106100000	183,900	-19210000	3,878,000	133,100	-91550000	-21060000
5	-252500	-299600000	-3742000	87,980	-27570000	-27430000	97,820	-83530000	-14150000
6	-152500	-287900000	94,630,000	17,240	-32480000	-56840000	72,820	-73250000	-7254000
7	-80370	-258500000	177,100,000	33,750	-34010000	-80650000	54,700	-60730000	510,800
8	-29540	-219500000	237,400,000	67,730	-32840000	-96380000	40,590	-46560000	9,196,000
9	4405	-179200000	277,300,000	88,090	-30110000	-1,04E + 08	29,720	-31540000	17,600,000
10	24,350	-140200000	303,600,000	96,460	-26690000	-1,06E + 08	21,240	-16380000	23,770,000
11	28,620	-100000000	318,600,000	90,950	-22560000	-1,04E + 08	15,470	-2044000	26,520,000
12	11,480	-55950000	318,700,000	68,210	-17220000	-97460000	14,410	10,430,000	25,880,000
13	-30130	-8386000	297,800,000	27,190	-10360000	-84910000	19,370	20,150,000	22,440,000
14	-96170	39,220,000	251,600,000	30,810	-2090000	-65720000	30,770	26,410,000	17,000,000
15	-182700	81,130,000	179,900,000	102,100	6,988,000	-40170000	47,790	28,640,000	10,330,000
16	-283500	110,800,000	88,100,000	180,900	15,940,000	-9993000	69,160	26,550,000	3,023,000
17	-390800	122,800,000	-14030000	260,600	23,690,000	21,780,000	93,560	20,230,000	-4502000
18	-495000	114,500,000	-113400000	333,600	29,190,000	51,370,000	119,000	10,270,000	-12120000
19	-597200	88,190,000	-197300000	400,700	32,120,000	75,120,000	146,100	-3040000	-20360000
20	-699100	50,970,000	-259200000	462,000	32,900,000	90,470,000	176,500	-19060000	-29220000
21	-796000	10,980,000	-300700000	514,800	32,270,000	97,560,000	208,900	-36700000	-37590000
22	-877600	-28800000	-328000000	554,900	30,660,000	98,970,000	239,100	-54710000	-43700000
23	-965200	-70970000	-344200000	590,900	28,710,000	95,920,000	275,200	-72970000	-46640000
24	-971200	-117700000	-343600000	580,700	23,630,000	88,880,000	284,400	-86910000	-45720000

**Table 5**  
Extrapolation points and mesh size.

Member	DNVGL [11]		IIW [10]	
	a (mm)	b (mm)	0.4 t (mm)	1.0 t (mm)
5110	31	101	16	40
5116	24	80	12	30
5112	23	76	10	25
4939	29	94	14	35
4940	38	124	22	55
4938	23	76	10	25

of IIW is more refined than the mesh of DNVGL and that the extrapolation points of IIW are closer to the regions of stress concentration. This is an important observation to be discussed in the results. In Fig. 6, the numerical models “DNVGL – Solid”, “DNVGL – Solid with Weld”, “IIW – Solid”, and “IIW – Solid with Weld”, using 8-noded three-dimensional solid element meshes with reduced integration (C3D8R), are shown.

**5. Results and discussion**

As recommended by DNVGL-RP-C203 [11], the principal stresses were extracted numerically at 16 points and then 8 hot-spot stresses were calculated for each brace, for all 24 steps. Figs. 7–12 show the comparison between the stresses obtained from the Eftymiou’s formulations proposed by DNVGL with the stresses obtained from the numerical simulations of the different meshes performed in this study. It is observed great conformity and compatibility between the numerical and the Eftymiou solutions in most points of the braces under analysis. This confirms the adjustment of the DNVGL equations to the results of the numerical studies. However, in some points of the intermediate braces, 5116 and 4940, the responses of the numerical models do not represent the Eftymiou’s results as in the external braces. The influence of the loading of the outer braces on the inner brace, the complexity of the loading and the geometry may justify the lack of compatibility at these points.

It is possible to notice that, in general, the numerical models accordingly IIW recommendations resulted in greater ranges than their corresponding ones according to the DNVGL models; for example, the curve of the solid model with mesh corresponding to IIW presents a greater stress amplitude than the curve of the same solid model in the DNVGL mesh. The same is observed for solid models with weld representation.

Mostly, the modules of the hot-spot stress obtained from the extrapolation method of IIW are higher than those obtained from the extrapolation method of DNVGL. This can be easily explained since the stress extraction points in the method proposed by IIW are closer to the stress concentration regions than the DNVGL stress extraction points (see Table 5). This behaviour demonstrates a greater

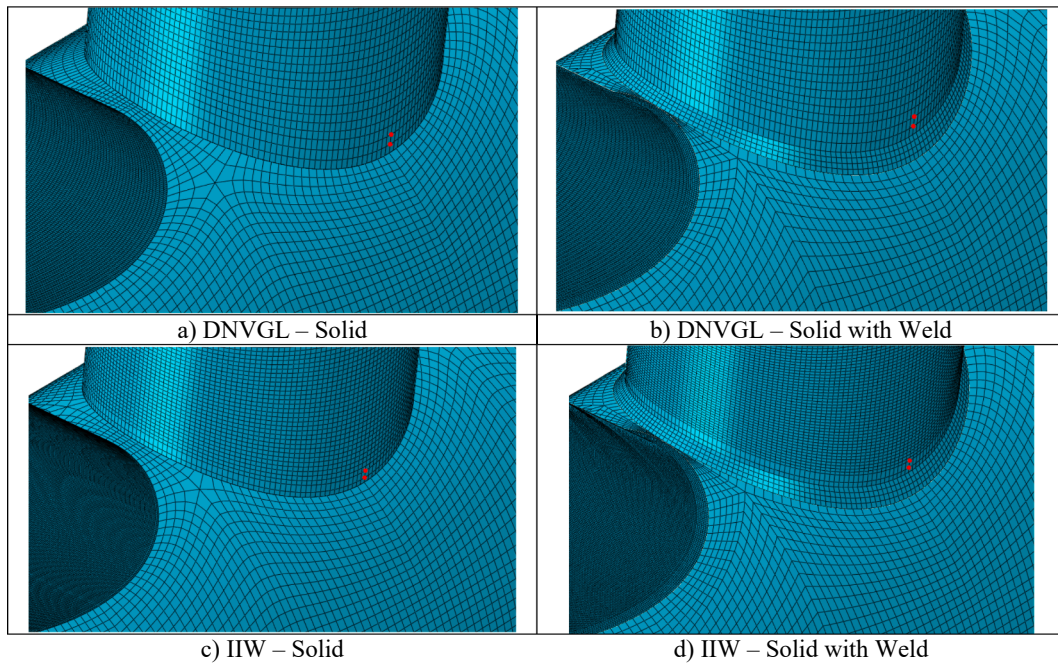


Fig. 6. Numerical models using 8-noded three-dimensional solid element meshes with reduced integration (C3D8R) – Plane YZ.

conservatism of the numerical hot-spot stress method according to the IIW recommendations, when compared to the DNVGL.

Regarding the influence of the weld on both IIW and DNVGL models, it is possible to observe a pattern in the movement of the curves in most parts of the points, which generates signs of good conformity of the results considering the models with and without representation of the weld. In these cases, no common behaviour was observed, such as a curve with higher and lower range, or an upper curve and a lower curve. As the stress ranges for both curves (with and without weld) are similar, it is indicated that the influence of the weld geometry in this configuration is not of great relevance in the numerical study.

The stress ranges for the two node planes simulated are shown in Figs. 13 and 14 and it is observed that in the YZ plane the stresses are significantly higher than in the XZ plane. For this reason, the YZ plane will be decisive for a future study regarding fatigue damage. The hot-spot stress range values at 8 points obtained for the braces 4938, 4940, 5112, 5116, and 5110, based on the analytical formulations present higher, similar, or lower values when compared to the numerical solutions, however, they exhibit curves of similar configuration. The exception is verified for the values of the hot-spot stress range at 8 points obtained for the brace 4939, since the curve of the hot-spot stress range at 8 points, obtained based on the analytical formulations (Efthymiou solutions) and numerical solutions present a different configuration. For the points 1, 2, 3, 4 and 5, the hot-spot stresses are underestimated; in the opposite locations, points 6, 7 and 8 overestimates the hot-spot stresses. When the comparison is made between the numerical solutions – DNVGL - Solid, DNVGL - Solid with Weld, IIW - Solid, and IIW - Solid with Weld – it is verified that the curves of the hot-spot stress range at 8 points present a configuration similar, but it is not clear which is the more or less conservative numerical solution. However, the numerical solution based on IIW seems to exhibit more conservative results when the analysis is done for all brace members.

Therefore, in order to evaluate and compare the mean value of the hot-spot stress range at eight points obtained by Efthymiou solutions and the numerical solutions of this research, the normalized difference index ( $e$ ) was considered and calculated. This variable was determined through Equation (11):

$$e(\%) = \frac{Efthymiou\ solution - numerical\ value}{Efthymiou\ solutions} \cdot 100\% \quad (11)$$

In Table 6, the normalized difference index was obtained for the mean value of the hot-spot stress range at eight positions when comparing analytical results and numerical solutions. As observed in Table 6, the numerical models based on the DNVGL and IIW recommendations presented a mean value of the normalized difference index for all braces in conjunction close to  $-8.9\%$ , leading to higher numerical values for the hot-spot stress range when compared with the results obtained based on the analytical solutions proposed by Efthymiou [27]. In general, for the numerical model “IIW – Solid”, the obtained hot-spot stress ranges for each brace under consideration led to higher normalized difference indexes when compared with the other models, “DNVGL – Solid with Weld”, “DNVGL – Solid”, and “IIW – Solid with Weld”. However, a good agreement can be considered between the models “DNVGL – Solid” and “DNVGL – Solid with Weld” based on the DNVGL standard and Efthymiou solutions. It is relevant to mention that the “DNVGL – Solid” model had the lowest computational cost due to two factors – the absence of the weld representation and coarser meshes, when compared with the IIW recommendations. The numerical models “DNVGL – Solid” and “DNVGL – Solid with weld” resulted in mean values of normalized difference index for all braces together of  $-7.09\%$  and  $3.96\%$ , respectively. The “IIW – Solid” and “IIW – Solid

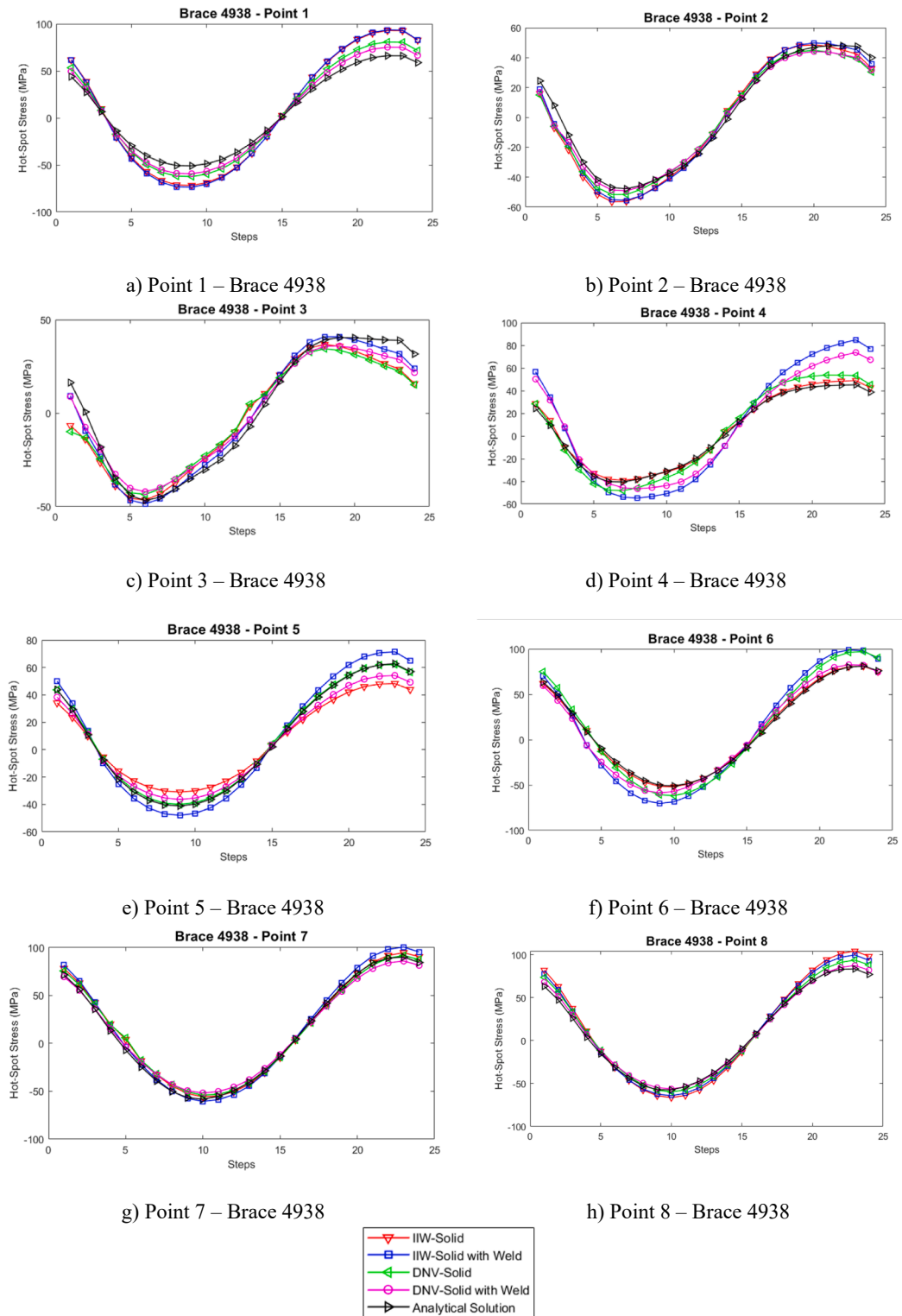
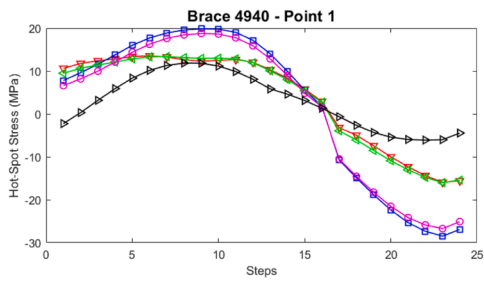
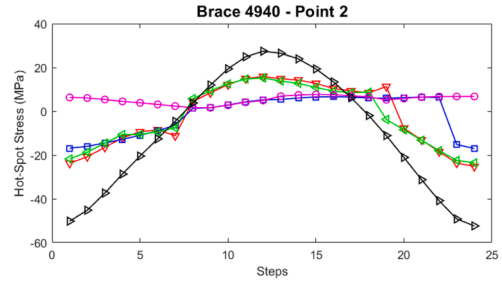


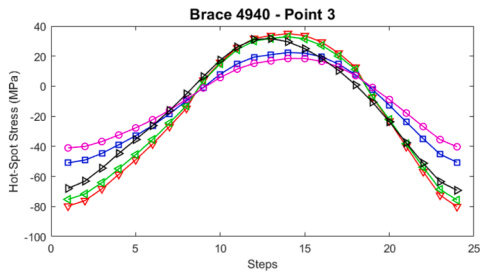
Fig. 7. Hot-Spot Stress in Brace 4938.



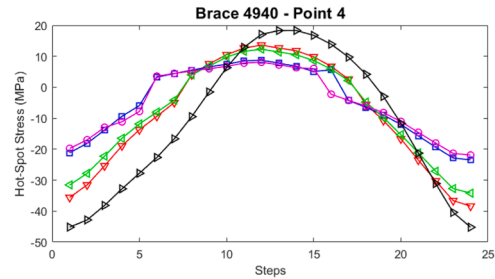
a) Point 1 – Brace 4940



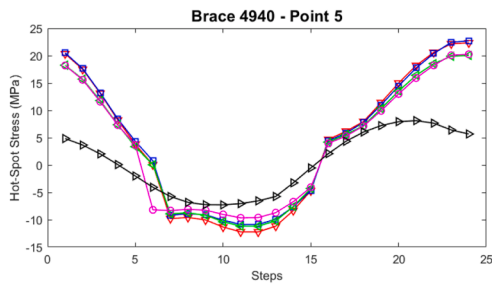
b) Point 2 – Brace 4940



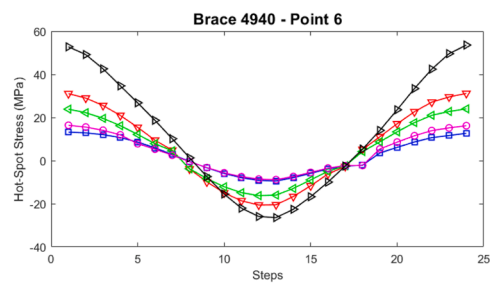
c) Point 3 – Brace 4940



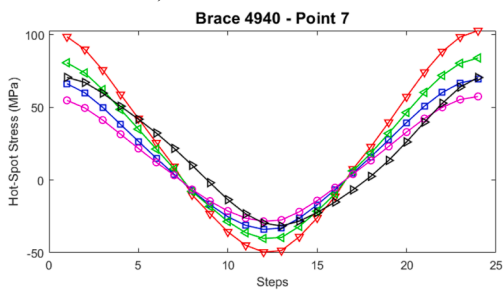
d) Point 4 – Brace 4940



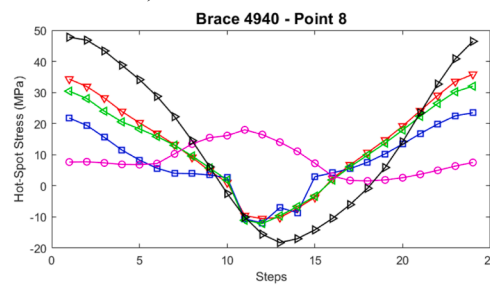
e) Point 5 – Brace 4940



f) Point 6 – Brace 4940



g) Point 7 – Brace 4940



h) Point 8 – Brace 4940

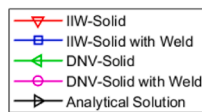


Fig. 8. Hot-Spot Stress in Brace 4940.

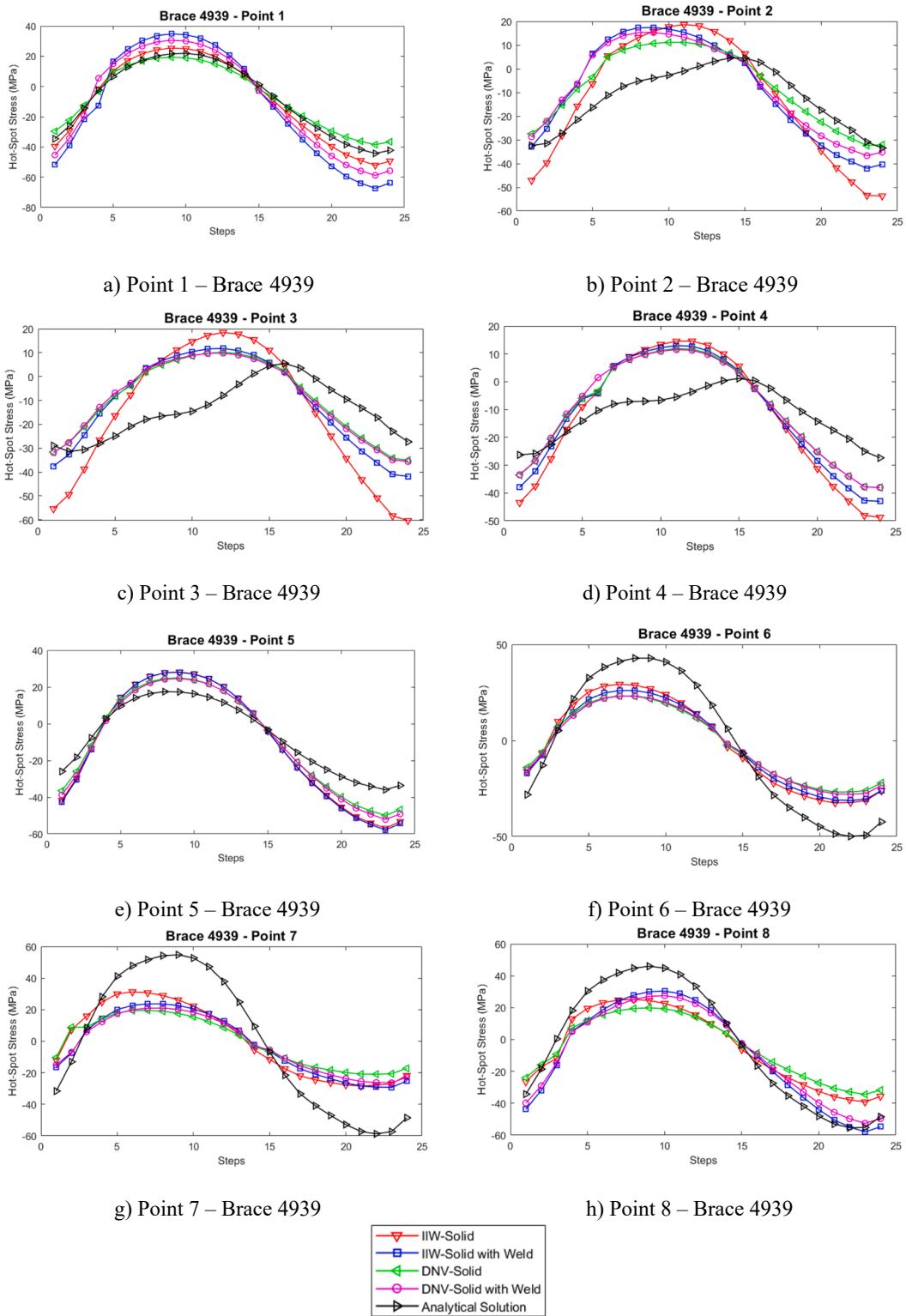


Fig. 9. Hot-Spot Stress in Brace 4939.

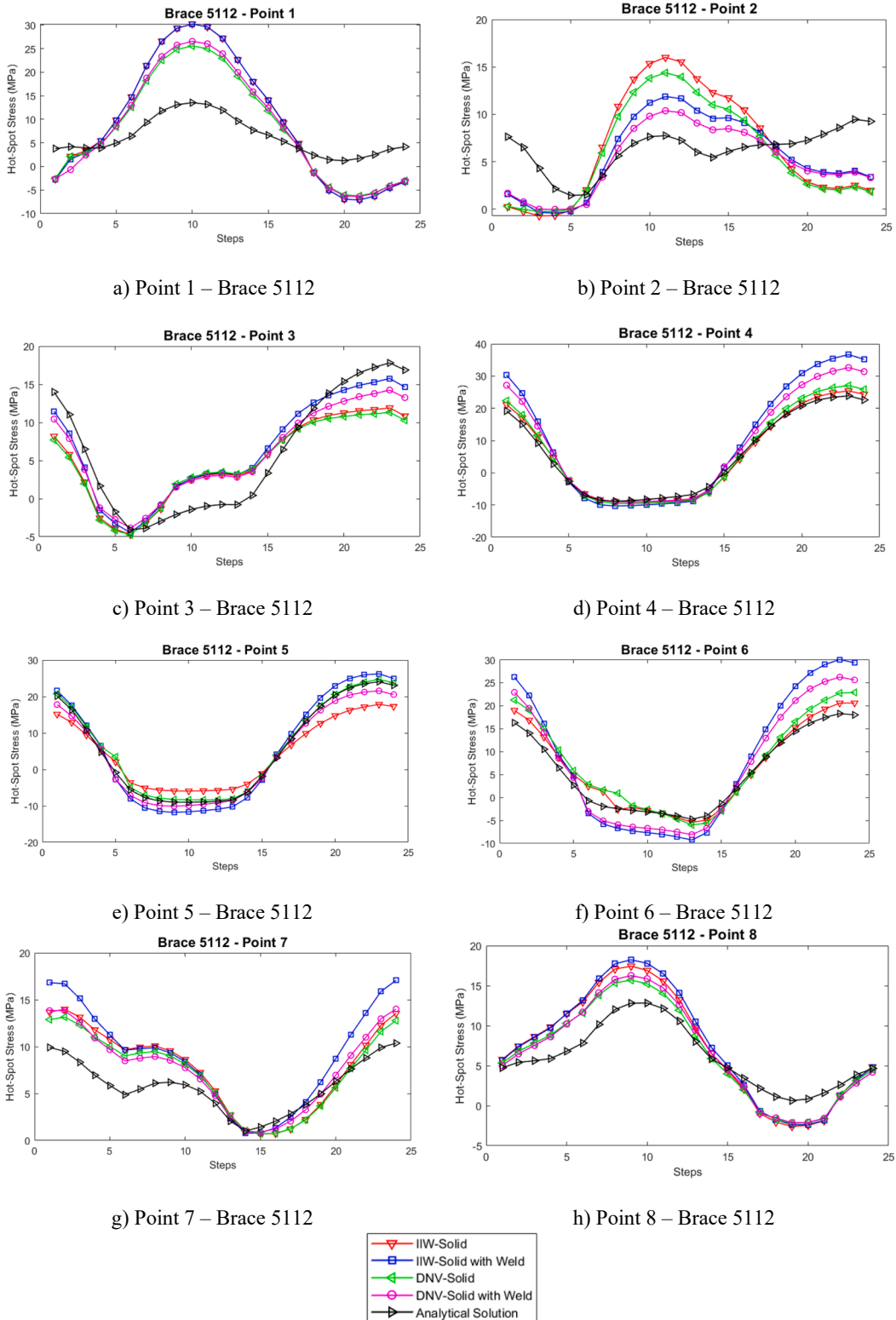


Fig. 10. Hot-Spot Stress in Brace 5112.

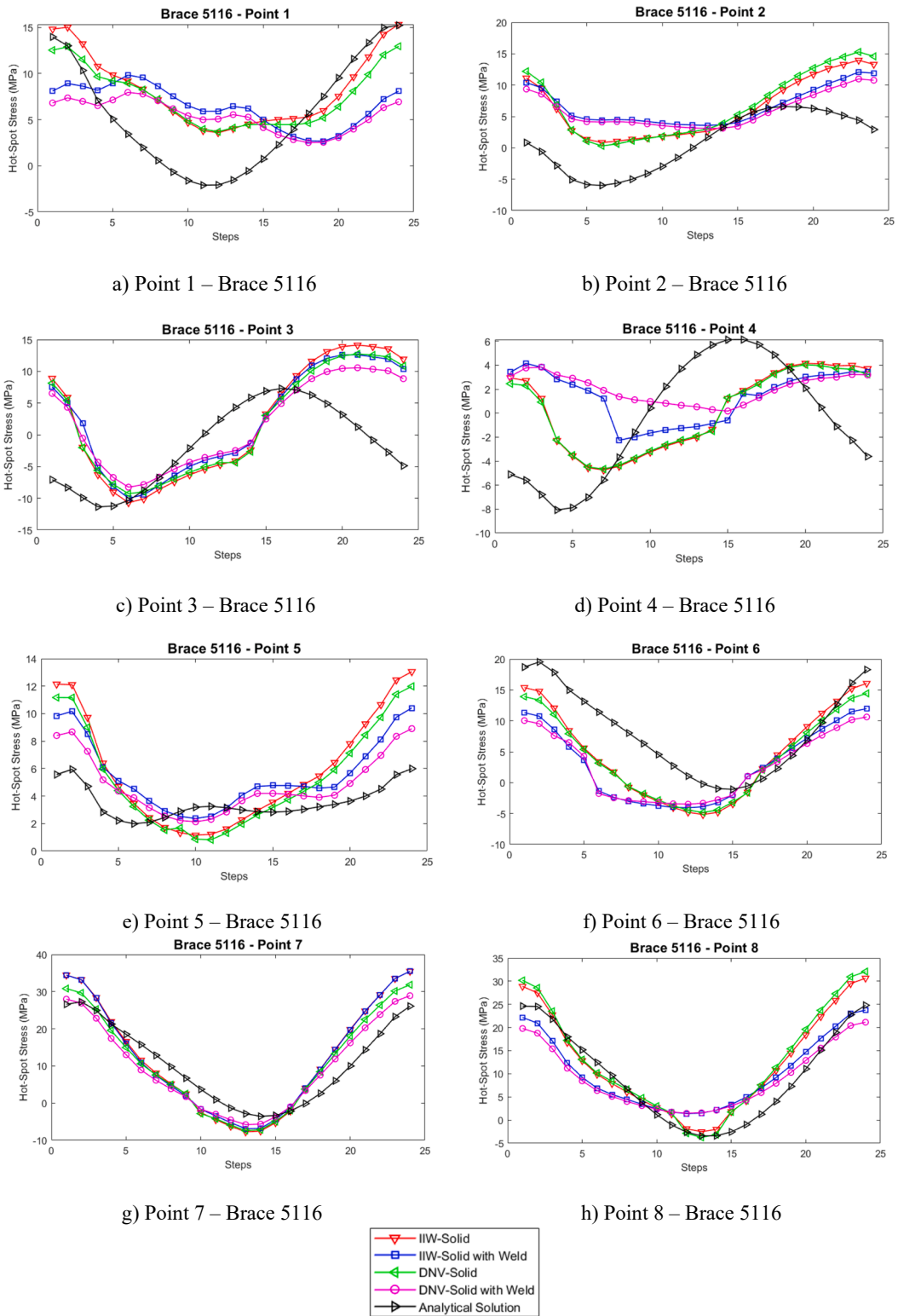
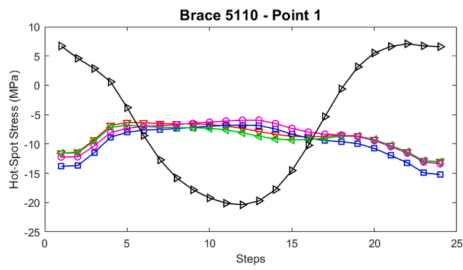
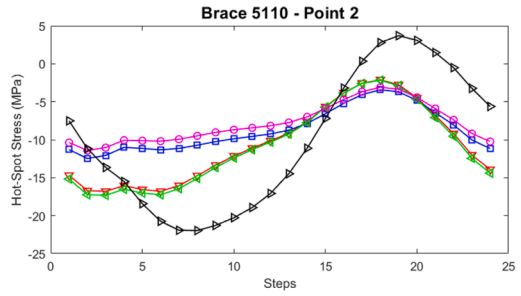


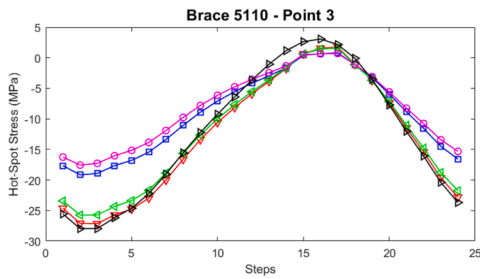
Fig. 11. Hot-Spot Stress in Brace 5116.



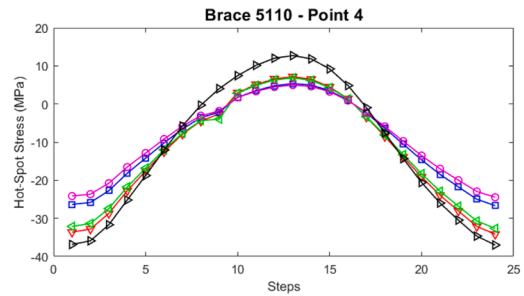
a) Point 1 – Brace 5110



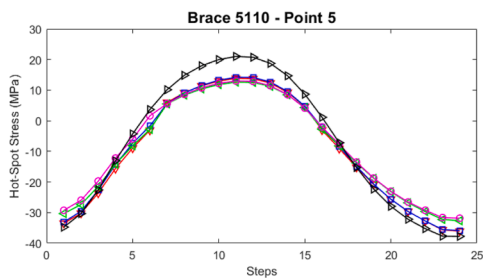
b) Point 2 – Brace 5110



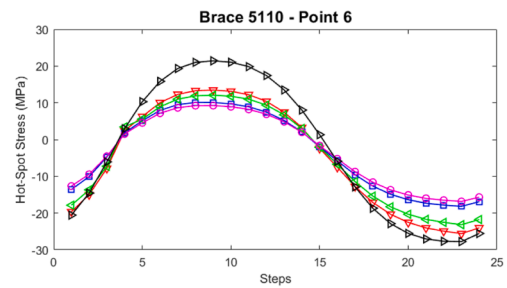
c) Point 3 – Brace 5110



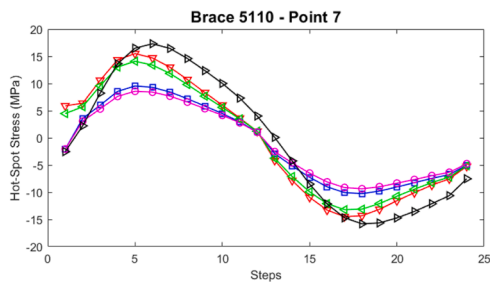
d) Point 4 – Brace 5110



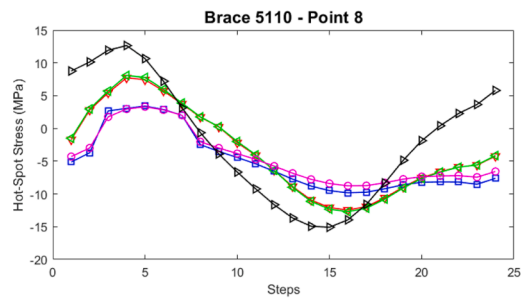
e) Point 5 – Brace 5110



f) Point 6 – Brace 5110



g) Point 7 – Brace 5110



h) Point 8 – Brace 5110

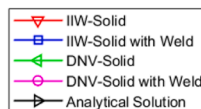


Fig. 12. Hot-Spot Stress in Brace 5110.

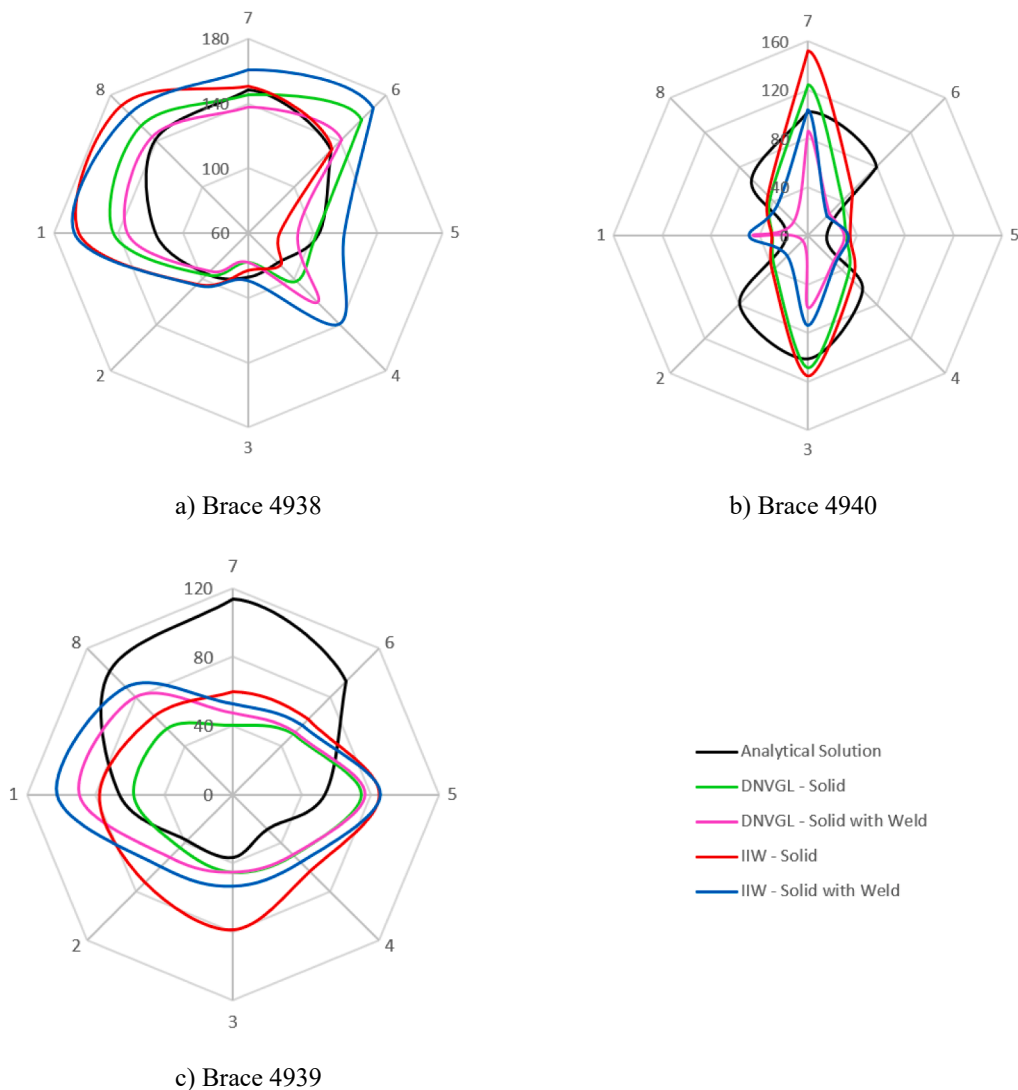


Fig. 13. Hot-Spot Stress Range (in MPa) – Plane YZ.

with weld” models exhibited mean values of normalized difference index for all braces in conjunction of  $-17.68\%$  and  $-11.59\%$ , respectively. In general, for the “DNVGL – Solid with weld” model, for each brace under consideration, the geometric effect of the welding led to lower hot-spot stress range values when compared to the obtained results based on the analytical solutions proposed by Efthymiou [27]. Otherwise, in general, for the “DNVGL – Solid”, “IIW – Solid” and “IIW – Solid with weld” models, the geometric effect of the welding led to higher hot-spot stress range values when compared to the obtained results based on the analytical solutions. The results obtained make it clear the need to improve the equations suggested by Efthymiou, since they were obtained using a finite element analysis based on 3-dimensional shell elements, where the weld was considered through diagonal elements, and in fewer conservative assumptions as indicated by HSE Offshore Technology Report [25]. As referred by HSE Offshore Technology Report [25], the results of hot-spot stresses and SCFs are almost always underestimated. In Table 6, the normalized difference indices precisely lead to this finding, whatever the approaches used (one exception), that is, finite element models using solid elements considering or not the weld in the modelling based on the DNVGL and IIW approaches. Therefore, based on the results obtained in this study using the hotspot stress method, new study opportunities appears aiming at characterizing the static and fatigue behaviours of welded joints using other methods such as strain energy density (SED) [46,47] and equilibrium equivalent structural stress approach [48], which have been increasingly used by the international scientific community due to the possibility to associate mesh insensitive procedures with coarse meshes as well as the possibility to explore the concept of a single master S-N curve.

However, some recommendations for obtaining the stress concentration factors (SCF) and/or hot-spot stress ranges of tubular welded joints, taking advantage of current computational capabilities, can be summarized:

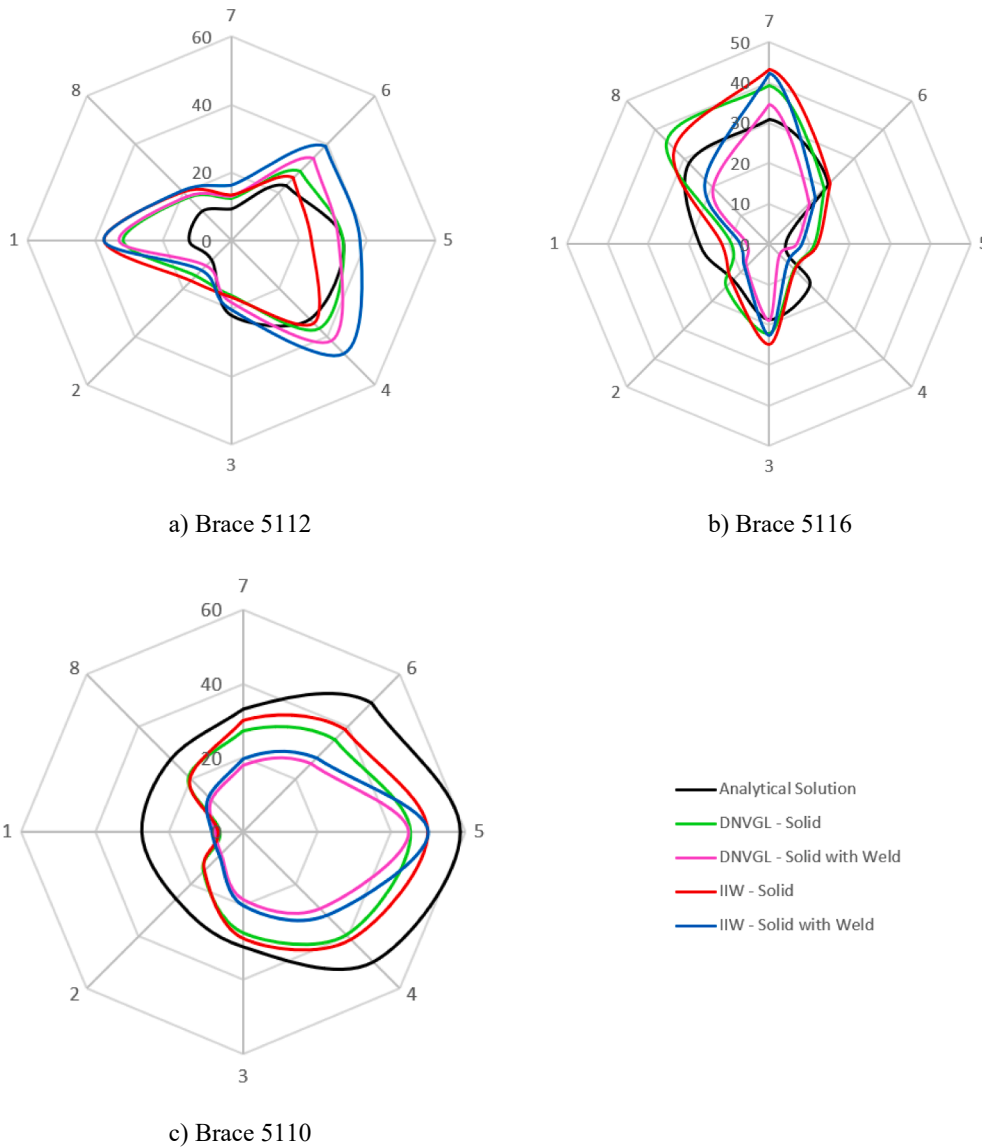


Fig. 14. Hot-Spot Stress Range (in MPa) – Plane XZ.

Table 6

Normalized difference index (%) obtained for the mean value of the hot-spot stress range at eight positions as a result of comparing numerical results with analytical solutions (note: negative values means higher numerical solution results).

Braces	Mean normalized difference index (%)			
	DNVGL - Solid	DNVGL - Solid with Weld	IIW - Solid	IIW - Solid with Weld
5110	30.58%	49.41%	26.81%	44.36%
5116	-22.25%	19.92%	-28.19%	3.68%
5112	-41.39%	-42.94%	-48.06%	-65.27%
4939	2.11%	-11.02%	-35.59%	-26.10%
4940	-4.31%	12.26%	-15.00%	-2.93%
4938	-7.13%	-3.86%	-6.02%	-23.27%
Mean	-7.06%	3.96%	-17.68%	-11.59%
	-8.09%			

- The calculation of the stress concentration factors (SCFs) and/or hot-spot stress ranges can be calculated based on Efthymiou analytical solutions and numerical solutions recommended by DNVGL and IIW;
- For design purposes, the most conservative values of SCFs and/or hot-spot stress ranges obtained based on analytical and numerical solutions should be considered;
- Whenever possible, the SCFs and/or hot-spot stress ranges should be supported based on experimental measurements to justify the results to be used in the fatigue damage calculations;
- Build numerical models of the tubular welded joints to estimate the local stresses and strains around the intersections between the arms and the chord of these joints, taking into account the boundary conditions coming from the global structural model and loads considered;
- Given the results obtained in this study, in the fatigue damage evaluation according to the design codes, reliability analyses should be considered based on practical recommendations since structures are almost always subjected to complex and extreme loads, where the effect of uncertainties in the loading is difficult to estimate.

Alternatively, fatigue damage assessment of tubular welded connections can be based on local approaches [144950] (e.g. local damage criteria based on fatigue properties of steels), total stress concept [51], or structural stress method [48], instead of using the hot-spot stress concept, taking advantage of current computational capabilities.

## 6. Conclusions

In this study, the evaluation and calculation of hot-spot stresses were presented following different methods, and technical recommendations for offshore jacket-type structures situated in the North Sea subjected to wave loads. Analytical and numerical methods proposed by DNVGL-RP-C203 [11] and numerical methods according to the IIW recommendations [10] were evaluated. To determine the hot-spot stresses, numerical models were developed using the ABAQUS finite element software considering a static analysis and linear-elastic material behaviour. In these models, the influence of the weld was also carefully investigated.

Based on the hot-spot stress curves presented, it is concluded that the influence of the weld geometry modelling in the structural stresses is generally modest. This can be justified by the simplifications adopted in the modelling of the weld since the different weld material properties and the weld penetration in the brace were not considered as in the studies of Hectors and De Weale [28]. The hot-spot stresses, in most cases, showed similar stress ranges, not implying significant changes due to the modelling of the weld geometry. However, for the numerical models with weld, the mean values of normalized difference index for all braces in conjunction, as a result of comparing numerical results with analytical solutions, are lower, but not as significant, when compared with results obtained from the numerical models without weld cord. For this reason, taking into account the results and simplifications adopted in the model, it is recommended to adopt the numerical model without weld in the prediction and studies of stresses since these models sometimes presented more conservative results than those with weld. Besides, the representation of the weld implies higher computational costs and may present difficulties regarding meshing. Further studies considering different geometries, welding materials, and residual stresses may confirm the relevance of the consideration of the weld in numerical models in the study of fatigue.

Regarding the mesh-size and extrapolation methods proposed by the IIW and DNVGL technical recommendations, it is reiterated that greater conservatism was observed in the modelling according to IIW method. However, the DNVGL extrapolation method is specific to tubular geometries of offshore structures. In this research, the hot-spot stresses estimated by the DNVGL technical recommendations can be considered close to the ones obtained by Efthymiou solutions. It should also be noted that this analysis is performed in comparison with Efthymiou formulations [27] based on finite element analysis using 3-dimensional shell elements and with few conservative assumptions as commented by HSE Offshore Technology Report [25], where the results obtained are almost always underestimated. In this way, it is necessary to observe with more numerical studies and compare with experimental measurements if the application of the IIW hot-spot stress method, as well as DNVGL approach, overestimate the stresses in offshore welded tubular joints, as this seems to be verified by the results obtained in this study. Therefore, the analytical formulations proposed by Efthymiou need to be improved and the approaches for obtaining the hot-spot stresses (mesh and extrapolation methods) clarified. Furthermore, static and fatigue characterization studies based on the strain energy density (SED) or structural stress approaches for welded joints, considering the complex and extreme loads as well as the effect of uncertainties in loading that these joints will be subject to, should be carried out. Then, a comparative analysis of the use of these approaches in relation to the use of the hot-spot stress concept must be done.

### *CRediT authorship contribution statement*

**Bianca Ávila:** Conceptualization, Validation, Formal analysis, Writing – original draft. **José Correia:** Conceptualization, Validation, Formal analysis, Writing – review & editing, Visualization, Supervision. **Hermes Carvalho:** Validation, Formal analysis, Writing – review & editing, Visualization, Supervision. **Nicholas Fantuzzi:** Formal analysis, Writing – review & editing, Visualization. **Abílio De Jesus:** Formal analysis, Writing – review & editing, Visualization. **Filippo Berto:** Formal analysis, Writing – review & editing, Visualization.

## Declaration of Competing Interest

The authors declare that they have no known competing financial interests or personal relationships that could have appeared to influence the work reported in this paper.

## Acknowledgments

This research work was supported by CAPES - PRINT Program (Coordination for the Improvement of Personnel of Graduation) and UFMG (Universidade Federal de Minas Gerais). Additionally, this research was also supported by the following grants: project grant (UTA-EXPL/IET/0111/2019) SOS-WindEnergy - Sustainable Reuse of Decommissioned Offshore Jacket Platforms for Offshore Wind Energy by national funds (PIDDAC) through the Portuguese Science Foundation (FCT/MCTES); base funding - UIDB/04708/2020 and programmatic funding - UIDP/04708/2020 of the CONSTRUCT - Instituto de I&D em Estruturas e Construções - funded by national funds through the FCT/MCTES (PIDDAC); AARM4 - High Strength Steels in Metalmechanics 4.0 (POCI-01-0247-FEDER-068492) funded by national funds through the PT2020/COMPETE; and, individual project grant (2020.03856.CEECIND), awarded to José A.F. O. Correia, by national funds (PIDDAC) through the Portuguese Science Foundation (FCT/MCTES). The authors would also like to thank all support by UT Austin Portugal Programme.

## References

- [1] F. Fu, *Design and Analysis of Tall and Complex Structures*, first ed., Butterworth-Heinemann, Elsevier, 2018.
- [2] M.L. Larsen, V. Arora, M. Lützen, R.R. Pedersen, E. Putnam, Fatigue life estimation of the weld joint in K-node of the offshore jacket structure using stochastic finite element analysis, *Mar. Struct.* 78 (2021) 103020, <https://doi.org/10.1016/j.marstruc.2021.103020>.
- [3] P.H. Wirsching, Fatigue reliability for offshore structures, *J. Struct. Eng.* 110 (10) (1984) 2340–2356.
- [4] C. Memos, K. Tzaniis, K. Zographou, Stochastic description of sea waves, *J. Hydraul. Res.* 40 (3) (2002) 265–274.
- [5] B. Yeter, Y. Garbatov, C. Guedes Soares, Evaluation of fatigue damage model predictions for fixed offshore wind turbine support structures, *Int. J. Fatigue* 87 (2016) 71–80.
- [6] M. Jimenez-Martinez, Fatigue of offshore structures: a review of statistical fatigue damage assessment for stochastic loadings, *Int. J. Fatigue* 132 (2020) 105327, <https://doi.org/10.1016/j.ijfatigue.2019.105327>.
- [7] X. Song, S. Wang, A novel spectral moments equivalence based lumping block method for efficient estimation of offshore structural fatigue damage, *Int. J. Fatigue* 118 (2019) 162–175.
- [8] M. Mlikota, S. Schmauder, Ž. Božić, Calculation of the Wöhler (S-N) curve using a two-scale model, *Int. J. Fatigue* 114 (2018) 289–297.
- [9] I. Losteberg, *Design of Marine Structure*, first ed., Cambridge University Press, 2017.
- [10] IIW International Institute of Welding. Recommendations for Fatigue Design of Welded Joints and Components, doc. XIII-2151r4-07/XV-1254r4-07, Paris, France, 2014.
- [11] DNV GL, DNVGL-RP-C203: Fatigue design of offshore steel structures, DNV GL, Oslo, Norway, 2016.
- [12] N. Shabakhly, D. Haselbozchaloe, J.A.F.O. Correia, Investigation on fatigue damage calibration factors in offshore structures, *Proc. Inst. Civ. Eng. Marit. Eng.* 174 (3) (2021) 65–80.
- [13] API, API-RP2A-WSD: Planning, designing, and constructing fixed offshore platforms-working stress design, API API, Washington, DC, USA, 2014.
- [14] A. Mourão, J.A.F.O. Correia, B.V. Ávila, C.C. de Oliveira, T. Ferradosa, H. Carvalho, J.M. Castro, A.M.P. De Jesus, A fatigue damage evaluation using local damage parameters for an offshore structure, *Proc. Inst. Civil Eng. - Maritime Eng.* 173 (2) (2020) 43–57.
- [15] H. Neuber, Theory of stress concentration for shear-strained prismatical bodies with arbitrary nonlinear stress-strain law, *J. Appl. Mech., Trans. ASME* 28 (4) (1960) 544–550.
- [16] W. Ramberg, W.R. Osgood, Description of stress-strain curves by three parameters, *NACA Tech.* 902 (1943).
- [17] L.F. Coffin, A study of the effects of the cyclic thermal stresses on a ductile metal, *Transl. ASME* 76 (1954) 931–950.
- [18] S.S. Manson, Behaviour of materials under conditions of thermal stress, *NACA TN-2933* (1954) 105.
- [19] J.D. Morrow, Cyclic plastic strain energy and fatigue of metals, in: *Int Frict Damp Cyclic Plast ASTM STP*, ed. B. Lazan, ASTM International, West Conshohocken, PA, 1965, pp. 45–87.
- [20] B. Nabuco, M. Tarpe, U.T. Tygesen, R. Brincker, Fatigue stress estimation of an offshore jacket structure based on operational modal analysis, *Shock Vib.* 2020 (2020) 1–12.
- [21] A.A. Toprac, L.A. Beale, Analysis of in-plane, T, Y and K welded tubular connections, *Welding Research Council*, 1967, p. 125.
- [22] J.B. Reber, Ultimate strength design of tubular joints, *Offshore Technol. Conf.* 2 (1972) 447–458.
- [23] W. Visser, On the structural design of tubular joints, *Offshore Technology Conference*, Houston, 1974.
- [24] J.G. Kuang, A.B. Potvin, R.D. Leick, Stress concentration in Tubular Joints, *Offshore Technology Conference*, Houston, 1975.
- [25] HSE Offshore Technology Report: "Stress Concentration Factors for Simple Tubular Joints: Assessment of Existing and Development of New Parametric Formulae," 1997.
- [26] A.B. Potvin, J.G. Kuang, R.D. Leick, J.L. Kahlich, Stress concentration in tubular joints, *Soc. Petrol. Eng. J.* 17 (1977) 287–299.
- [27] M. Efthymiou, Development of SCF formulae and generalised influence functions for use in fatigue analysis, *Offshore Tubular Joints* (1988).
- [28] K. Hectors, W. De Waele, Influence of weld geometry on stress concentration factor distributions in tubular joints, *J. Constr. Steel Res.* 176 (2021) 106376, <https://doi.org/10.1016/j.jcsr.2020.106376>.
- [29] AWS Structural Welding Code, D1.1 Edition (2015).
- [30] CIDETC Design Guide No. 8 (2000).
- [31] M. Haghpanahi, H. Pirali, Hot spot stress determination for a tubular T-joint under combined axial and bending loading, *Int. J. Eng. Sci.* 17 (2006) 21–28.
- [32] Y. Yin, X. Liu, P. Lei, L. Zhou, Stress concentration factor for tubular CHS-to-RHS Y-joints under axial loads, *J. Constr. Steel Res.* 148 (2018) 768–778.
- [33] S. Bao, X. Li, B. Wang, Study on hot spot stress of three-planar tubular Y-joints under combined axial loads, *Thin-Walled Struct.* 140 (2019) 478–494.
- [34] S. Bao, W. Wang, Y.H. Chai, X. Li, Hot spot stress parametric equations for three-planar tubular Y-joints subject to in-plane bending moment, *Thin-Walled Struct.* 149 (2020) 106648, <https://doi.org/10.1016/j.tws.2020.106648>.
- [35] S. Bao, W. Wang, X. Li, H. Zhao, Hot-spot stress caused by out-of-plane bending moments of three planar tubular Y-joints, *Appl. Ocean Res.* 100 (2020) 102179, <https://doi.org/10.1016/j.apor.2020.102179>.
- [36] E.O. Oshogbunu, Y.C. Wang, T. Stallard, A new method for calculating hot-spot stress in gap DKK CHS joints under arbitrary loading, *Eng. Struct.* 210 (2020) 110366, <https://doi.org/10.1016/j.engstruct.2020.110366>.
- [37] E.O. Oshogbunu, Y.C. Wang, T. Stallard, Reliability and applications of a new design method for calculating hot-spot stress in CHS double K-joints under arbitrary combined loading, *Structures* 29 (2021) 1610–1626.
- [38] A. Aidibi, S. Babamohammadi, N. Fatnuzzi, J.A.F.O. Correia, L. Manuel, Stress concentration factor evaluation of offshore tubular KT joints based on analytical and numerical solutions: comparative study, *Pract. Period. Struct. Des. Constr.* 26 (4) (2021) 04021047.

- [39] A. Mourão, Fatigue analysis of a jacket-type offshore platform based on local approaches, Dissertação, University of Porto, Porto, Portugal, 2018, p. 139.
- [40] M.K.K. Lee, Estimation of stress concentrations in single-sided welds in offshore tubular joints, *Int. J. Fatigue* 21 (1999) 895–908.
- [41] D.S. Simulia, ABAQUS 6.14 User's Manual, Dassault Systems, 2014.
- [42] M.A. Lotfollahi-Yaghin, H. Ahmadi, Effect of geometrical parameters on SCF distribution along the weld toe of tubular KT-joints under balanced axial loads, *Int. J. Fatigue* 32 (4) (2010) 703–719.
- [43] S.P. Chiew, C.K. Soh, T.C. Fung, A.K. Soh, Numerical study of multiplanar tubular DX-joints subject to axial loads, *Comput. Struct.* 72 (6) (1999) 749–761.
- [44] DNV GL, DNV-RP-C205: Environmental conditions and environmental loads, DNV GL, Oslo, Norway, 2014.
- [45] D.S. Saini, D. Karmakar, S. Ray-Chaudhuri, A review of stress concentration factors in tubular and non-tubular joints for design of offshore installations, *J. Ocean. Eng. Sci.* 1 (3) (2016) 186–202.
- [46] F. Berto, P. Lazzarin, A review of the volume-based strain energy density approach applied to V-notches and welded structures, *Theor. Appl. Fract. Mech.* 52 (3) (2009) 183–194.
- [47] F. Berto, P. Lazzarin, Recent developments in brittle and quasi-brittle failure assessment of engineering materials by means of local approaches, *Mater. Sci. Eng. R: Rep.* 75 (1) (2014) 1–48.
- [48] G. Alencar, J.K. Hong, A. de Jesus, J.G.S. da Silva, R. Calçada, The master S-N curve approach for fatigue assessment of welded bridge structural details, *Int. J. Fatigue* 152 (2021), 106432.
- [49] C.O. Viana, H. Carvalho, J. Correia, P.A. Montenegro, R.P. Heleno, G.S. Alencar, A.M.P. Jesus, R. Calçada, Fatigue assessment based on hot-spot stresses obtained from the global dynamic analysis and local static sub-model, *Int. J. Struct. Integr.* 12 (1) (2021) 31–47.
- [50] Z. Liu, J. Correia, H. Carvalho, A. Mourão, A. Jesus, R. Calçada, F. Berto, Global-local fatigue assessment of an ancient riveted metallic bridge based on submodelling of the critical detail, *Fatigue Fract. Eng. Mater. Struct.* 42 (2) (2019) 546–560.
- [51] Y. Qin, H. den Besten, S. Palkar, M.L. Kaminski, Mid- and high-cycle fatigue of welded joints in steel marine structures: effective notch stress and total stress concept evaluations, *Int. J. Fatigue* 142 (2021), 105822.